

Real-time Dispatchable Region of Active Distribution Networks Based on a Tight Convex Relaxation Model

Wenjing Huang, Zhigang Li, *Member, IEEE*, Mohammad Shahidehpour, *Fellow, IEEE*, and J. H. Zheng, *Member, IEEE*

Abstract—The uncertainty in distributed renewable generation poses security threats to the real-time operation of distribution systems. The real-time dispatchable region (RTDR) can be used to assess the ability of power systems to accommodate renewable generation at a given base point. DC and linearized AC power flow models are typically used for bulk power systems, but they are not suitable for low-voltage distribution networks with large r/x ratios. To balance accuracy and computational efficiency, this paper proposes an RTDR model of AC distribution networks using tight convex relaxation. Convex hull relaxation is adopted to reformulate the AC power flow equations, and the convex hull is approximated by a polyhedron without much loss of accuracy. Furthermore, an efficient adaptive constraint generation algorithm is employed to construct an approximate RTDR to meet the requirements of real-time dispatch. Case studies on the modified IEEE 33-bus distribution system validate the computational efficiency and accuracy of the proposed method.

Index Terms—convex hull relaxation, distribution system, real-time dispatchable region, renewable generation, uncertainty

NOMENCLATURE

A. Indices and Sets

- $(\cdot)_j$ Symbol associated with bus j .
- $(\cdot)_{ij}$ Symbol associated with the line from bus i to bus j .
- $W(j)$ Set of renewable energy units connected to bus j .

B. Input Parameters

- p_j^d Fixed active power demand at bus j .
- p_j^g Active generation at bus j .
- q_j^d Fixed reactive power demand at bus j .
- q_j^g Reactive generation at bus j .

- r_{ij} Resistance of the line from bus i to bus j .
- \bar{S}_{ij} Maximum apparent power on the line from bus i to bus j .
- w_n Actual output of renewable generator n .
- w_n^e Predicted output of renewable generator n .
- x_{ij} Reactance of the line from bus i to bus j .

C. Decision Variables

- ℓ_{ij} Squared line current magnitude on the line from bus i to bus j .
- p_j^c Rescheduling active generation at bus j .
- P_{ij} Active power flow on the line from bus i to bus j .
- q_j^c Rescheduling reactive generation at bus j .
- Q_{ij} Reactive power flow on the line from bus i to bus j .
- v_i Squared voltage magnitude at bus i .
- Δw_n Deviation between the predicted output and actual output of renewable generator n .
- y Combination of all decision variables except Δw .

I. INTRODUCTION

THE large-scale utilization of renewable energy can remarkably reduce the dependence on fossil fuel and thereby help alleviate air pollution. However, the variability also increases the risks of power system dispatch infeasibility, in which case the generation would fail to balance the load or the transmission network would be congested [1]. Therefore, sufficient power system flexibility is required to cope with these challenges. Reference [2] provides a comprehensive understanding of the flexibility of power systems, particularly when large-scale volatile renewable generation is integrated. Moreover, a geometric interpretation is given by straightforward visualization in [2] to express the effect of various resources on grid-side flexibility.

Recently, the dispatchable region in [3]-[5] replaced the probability distribution function (PDF) commonly used in the past to characterize the ability of a power system to

accommodate fluctuating renewable energy. A concept related to the dispatchable region is the do-not-exceed (DNE) limit [6], which defines the maximum rectangular security region for renewable energy generation (REG). A data-driven method is proposed in [7] to construct DNE limits to maximize the utilization of REG. However, the box-type DNE is an inner approximation of dispatchable region, which often appears to be conservative. As an alternative, polyhedral and elliptical sets [8], [9] are developed to describe the ranges of uncertain parameters. However, the DNE region cannot accurately describe the real ability of a power system to accommodate fluctuations. Therefore, characterizing the exact dispatchable region from a theoretical perspective is attractive.

The concept of dispatchable region is formally proposed for transmission systems based on a DC power flow model in [3]. Reference [4] defines the real-time dispatchability based on [3]. In real-time dispatch (RTD), given that the current operating point is known, all constraints in the RTD are projected onto the space of uncertainty parameters, yielding the dispatchable region. Mathematically, the real-time dispatchable region (RTDR) is presented as a polytope constructed by solving a series of mixed-integer linear programming (MILP) problems [4]. The shape of the RTDR can be actively controlled by energy-reserve co-dispatch [5]. However, due to the short time scale of RTD, contingencies are not considered. These contingencies can be considered in the unit commitment [10], [11] and economic dispatch [12], [13]. References [3]-[5] use a DC power flow model without considering the voltage magnitude and reactive power, which may generate unsafe operating points in the RTDR. A dispatchable region model based on linearized AC power flow is proposed in [14], which provides a good approximation for high-voltage transmission networks.

The mentioned references except for [14] adopt a DC power flow model, whereas reference [14] adopts a linearized AC power flow model. However, AC power flow equations are inherently nonlinear. For a distribution network with high r/x ratios of transmission lines, the linearization of the power flow model disregards nonlinearity details and leads to infeasible power flow profiles. In this context, the nonlinearity of power flow should be properly addressed.

To tackle these issues, this paper focuses on the RTDR of volatile REG in distribution networks considering AC power flow. The branch flow model (BFM) known as *DistFlow* is adopted to describe the radial distribution network with the phase angles eliminated [15]. Because the BFM is essentially an AC power flow model, it is nonconvex and nonlinear. The methods of constructing the convex inner approximation of the solvable region for power flow [16]-[17] usually lead to overly conservative results. Therefore, we adopt the convex outer approximation to the nonconvex feasible region, which is a more reasonable method. A relaxed and convex BFM is proposed in [18] and [19], which is always accurate in the radial network as long as the power of the load does not have an upper limit. The convex hull formulation of the nonconvex quadratic equation in the BFM is constructed in [20]. The convex hull is composed of a second-order cone (SOC) and a linear inequality,

which has been proved and validated in [20] to be the tightest convex outer approximation of the nonconvex quadratic equation in the BFM. To the best of our knowledge, there is no research on using convex hulls in the RTDR.

In this paper, we make the first attempt to use convex hulls in RTDR. Specific contributions of this paper are summarized as follows.

1) An RTDR model suitable for distribution networks is devised based on a BFM. A tighter convex outer approximation of the RTDR is obtained by using the convex hull of the quadratic equation. Compared with those in the existing work, the proposed model contains all feasible operating points of nodal power injections in a power system, even in power systems with large differences in r/x ratios of the lines.

2) A high-precision linear convex outer approximation of the RTDR is developed. An adaptive constraint generation algorithm is exploited to construct the boundaries of the proposed RTDR, the computational efficiency of which is reliable for real-time dispatch. In particular, a polyhedral outer approximation is used to address the SOC constraint in the convex hull as well as the quadratic inequality constraint. The case study also shows that even if the sufficient conditions for the exact convex relaxation of BFM are not satisfied, acceptable result is still available.

The rest of this paper is organized as follows. The RTDR in distribution system is defined and formulated in Section II. The tight convex relaxation of the RTDR and the adaptive constraint generation (Ad-CG) algorithm are presented in Section III. Case studies on the modified IEEE 33-bus system are reported in Section IV. Conclusions are given in Section V.

II. DEFINITION AND FORMULATION OF THE RTDR IN A DISTRIBUTION SYSTEM

The volatile REG affects the power balance of RTD in a power system. In the current dispatch interval, the pre-dispatch strategy of traditional generators is denoted by $\{p^g, q^g\}$, the output of renewable generators may deviate from the predicted value w^e , and their actual output is assumed to be $w = w^e + \Delta w$. Once the output deviation Δw of REG is observed, the rescheduling strategy $\{p^c, q^c\}$ is implemented to restore the system to a secure operating state, and the output of the traditional generators is changed to $\{p^g + p^c, q^g + q^c\}$. Due to the limited ramping capability of generators, the system cannot accommodate arbitrarily large ranges of REG fluctuation. The RTDR can be expressed in the following abstract form:

$$W(p^g, q^g, w^e) = \{\Delta w \mid \exists y: f(\Delta w, y) \leq 0\} \quad (1)$$

where $f(\Delta w, y) \leq 0$ represents the power flow equations and operating limits of the power system, and y represents the variables related to corrective actions that rebalance the power system. Δw is a parameter of W .

Here, the constraints $f(\Delta w, y) \leq 0$ of the distribution system include the following:

$$p_j^g + p_j^c - p_j^d = \sum_{k:j \rightarrow k} P_{jk} - (P_{ij} - r_{ij} \ell_{ij}) - \sum_{n \in W(j)} w_n \quad (2)$$

$$q_j^g + q_j^c - q_j^d = \sum_{k:j \rightarrow k} Q_{jk} - (Q_{ij} - x_{ij} \ell_{ij}) \quad (3)$$

$$v_j = v_i - 2(r_{ij} P_{ij} + x_{ij} Q_{ij}) + (r_{ij}^2 + x_{ij}^2) \ell_{ij} \quad (4)$$

$$P_{ij}^2 + Q_{ij}^2 = v_i \ell_{ij} \quad (5)$$

$$\underline{p}_j^g \leq p_j^g + p_j^c \leq \bar{p}_j^g, \underline{q}_j^g \leq q_j^g + q_j^c \leq \bar{q}_j^g \quad (6)$$

$$w_n = w_n^c + \Delta w_n \leq \bar{w}_n \quad (7)$$

$$0 \leq |p_j^c| \leq Ramp_j \quad (8)$$

$$0 \leq \ell_{ij} \leq \bar{\ell}_{ij} \quad (9)$$

$$\underline{v}_j \leq v_j \leq \bar{v}_j \quad (10)$$

$$P_{ij}^2 + Q_{ij}^2 \leq \bar{S}_{ij}^2 \quad (11)$$

$$P_{ij} \geq 0, Q_{ij} \geq 0 \quad (12)$$

where the subscript i denotes the index of the bus and (i,j) denotes the directed branch linking buses i and j . The superscripts g, c, and d represent the pre-dispatch output of the traditional generator, the change in the rescheduled output of the traditional generator, and the load on the bus, respectively. Constraints (2)-(5) represent the BFM of the distribution network based on the *DistFlow* model [15]. Constraints (2) and (3) are nodal active and reactive power balancing conditions. Constraint (4) describes the voltage drop on each line. Constraint (5) describes the apparent power flow at the from-bus of each line. Constraint (6) is the capacity restriction on the traditional generator. Constraint (7) is the active output of REG, where \bar{w}_n is the maximum output of the renewable resources. Constraint (8) stipulates that the regulation power of a traditional generator is subjected to the ramping capacity. Constraints (9), (10), and (11) are the line current capacity, voltage magnitude constraint, and apparent power flow limit of the distribution lines, respectively. Constraint (12) prevents the backflow of power on the feeders.

The load of the current system and the predicted active power output w^c of REG are assumed to be predefined by forecasting algorithms. Then, the current pre-dispatch strategy $\{p^g, q^g\}$ can be calculated. y includes all variables except p^g, q^g and Δw in constraints (2)-(12).

III. TIGHT CONVEX RELAXATION OF THE RTDR AND ITS SOLUTION

The BFM (2)-(5) is nonconvex and nonlinear, resulting in a nonconvex RTDR. In this section, to make the construction of the RTDR tractable, a convex hull of the original RTDR is developed to provide an outer approximation of the original RTDR. This convex hull is further relaxed into a polyhedral RTDR, which can be readily constructed using the Ad-CG algorithm.

A. Polyhedral Outer Approximation Based on Convex Hull Relaxation

The convex hull (CH), analytically proved and geometrically verified in [20], is adopted to outer approximate the RTDR. Let Ω_0 denote the feasible set described by the quadratic equality (5) and (9)-(11) for each branch (i,j) and Ω_1 be the CH of Ω_0 , which are formulated as follows:

$$\Omega_0 = \{\mathbf{x}_{ij} \mid (5) \text{ and } (9)-(11) \text{ hold}\} \quad (13)$$

$$\Omega_1 = \text{CH}(\Omega_0) = \left\{ \mathbf{x}_{ij} \mid \begin{cases} \|\mathbf{A}\mathbf{x}_{ij}\|_2 - \mathbf{b}^T \mathbf{x}_{ij} \leq 0 \\ \mathbf{c}_{ij}^T \mathbf{x}_{ij} - \mathbf{d}_{ij} \leq 0 \\ \mathbf{x}_{ij} \in (10)-(12) \end{cases} \right\} \quad (14)$$

where $\mathbf{x}_{ij} = [P_{ij}, Q_{ij}, \ell_{ij}, v_i]^T$, $\mathbf{A} = \text{diag}([\sqrt{2}, \sqrt{2}, 1, 1]^T)$ and $\mathbf{b} = [0, 0, 1, 1]^T$. $\|\mathbf{A}\mathbf{x}_{ij}\|_2 - \mathbf{b}^T \mathbf{x}_{ij} \leq 0$ in Ω_1 represents the SOC of quadratic equality (5) in the following form:

$$P_{ij}^2 + Q_{ij}^2 \leq v_i \ell_{ij}. \quad (15)$$

which is the convex relaxation of (5).

The values of the coefficient vectors in $\mathbf{c}_{ij}^T \mathbf{x}_{ij} - \mathbf{d}_{ij} \leq 0$ depend on specific constraints. When $\bar{S}_{ij}^2 \leq \bar{\ell}_{ij} \bar{v}_i$, the branch flow is bounded by (11), with (9) being redundant; then, we have $\mathbf{c}_{ij} = [0, 0, \underline{v}_i \bar{v}_i, \bar{S}_{ij}^2]^T$ and $\mathbf{d}_{ij} = (\underline{v}_i + \bar{v}_i) \bar{S}_{ij}^2$. When $\bar{S}_{ij}^2 \geq \bar{\ell}_{ij} \bar{v}_i$, we have $\mathbf{c}_{ij} = [0, 0, \bar{v}_i, \bar{\ell}_{ij}]^T$ and $\mathbf{d}_{ij} = \bar{\ell}_{ij} \bar{v}_i + \bar{S}_{ij}^2$. When $\bar{S}_{ij}^2 \geq \bar{\ell}_{ij} \bar{v}_i$, (11) is redundant. Constraint (11) usually dominates (9) for long transmission lines, and the converse may occur for distribution feeders.

The relation between Ω_0 and Ω_1 is shown in Fig. 1. The extreme points of the CH belong to its original nonconvex set.

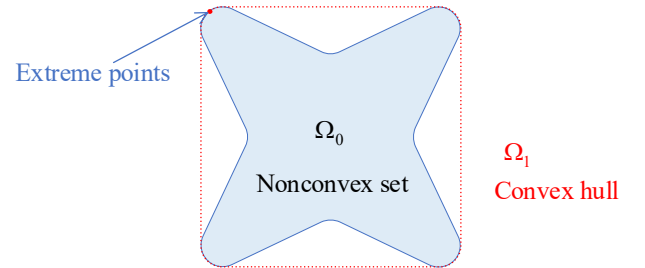


Fig. 1. Illustration of the advantages of the CH

The sufficient conditions for the exact convex relaxation of the BFM in radial network are summarized in [21]:

- 1) *Power injections*: The constraints on active and reactive power injections are not binding at either end of the line.
- 2) *Voltage magnitudes*: The upper bounds on voltage magnitudes are not binding.

Since CH relaxation introduces an SOC, the boundary of the obtained RTDR is still nonlinear. To construct the RTDR with linear boundaries, the technique in [22] is used to generate the polyhedral outer approximation of the RTDR. The rotated SOC

(15) in \mathbb{R}^4 is split into a combination of two standard SOCs in \mathbb{R}^3 as follows:

$$m_{ij} \geq \sqrt{P_{ij}^2 + Q_{ij}^2} \quad (16)$$

$$m'_{ij} \geq \sqrt{P'_{ij}{}^2 + Q'_{ij}{}^2} \quad (17)$$

$$Q'_{ij} = m_{ij} = \frac{v_i - \ell_{ij}}{2} \quad (18)$$

$$m'_{ij} = \frac{v_i + \ell_{ij}}{2} \quad (19)$$

where m_{ij}, m'_{ij}, P'_{ij} and Q'_{ij} are auxiliary variables. Then, auxiliary variables $P_{ij,n}$ and $Q_{ij,n}$ ($n=1, \dots, k$) are introduced to obtain the polyhedral outer approximation of standard SOC (16) in \mathbb{R}^3 in the following form:

$$P_{ij,n+1} - P_{ij,n} \cos \frac{\pi}{2^n} - Q_{ij,n} \sin \frac{\pi}{2^n} = 0, \quad n = 0, \dots, k-1 \quad (20)$$

$$Q_{ij,n+1} - Q_{ij,n} \cos \frac{\pi}{2^n} + P_{ij,n} \sin \frac{\pi}{2^n} \geq 0, \quad n = 0, \dots, k-1 \quad (21)$$

$$Q_{ij,n+1} + Q_{ij,n} \cos \frac{\pi}{2^n} - P_{ij,n} \sin \frac{\pi}{2^n} \geq 0, \quad n = 0, \dots, k-1 \quad (22)$$

$$P_{ij,k} \cos \frac{\pi}{2^k} + Q_{ij,k} \sin \frac{\pi}{2^k} - m_{ij} = 0 \quad (23)$$

Note that equations (20) and (23) can eliminate the auxiliary variables $P_{ij,n}$ ($n=1, \dots, k$) and $Q_{ij,k}$ in inequalities (21) and (22). In this way, we obtain $2k$ inequalities with $k+2$ variables that are stylized as

$$g(m_{ij}, P_{ij}, Q_{ij}, Q_{ij,1}, \dots, Q_{ij,k-1}) \leq 0 \quad (24)$$

Similarly, the standard SOC (17) in \mathbb{R}^3 can also be approximated as a set of $2k$ inequalities with $k+2$ variables:

$$g(m'_{ij}, P'_{ij}, Q'_{ij}, Q'_{ij,1}, \dots, Q'_{ij,k-1}) \leq 0 \quad (25)$$

The set of inequalities (24) constructs a high-dimensional polyhedron space, whose projection on the hyperplane of the SOC (16) is a tight outer approximation of the SOC. The relaxation accuracy $\varepsilon_1 = \cos^{-1}(\pi/2^k) - 1$ satisfies [23]

$$1 + \varepsilon_1 \geq \frac{\sqrt{P_{ij}^2 + Q_{ij}^2}}{m_{ij}} \quad (26)$$

Suppose that the relaxation accuracy of the polyhedral approximation (25) is ε_2 ; then, the overall approximation accuracy ε of the rotated SOC (15) is

$$\varepsilon = (1 + \varepsilon_1)(1 + \varepsilon_2) - 1 \quad (27)$$

The larger k is, the higher the overall approximation accuracy that can be obtained.

B. Linear Relaxation of the Quadratic Inequality Constraint

The quadratic inequality constraint (11) is identified as a type of power circle constraint, which can also be approximated via polyhedral constraints.

For a circle with a radius of R , the area inside the circle $x^2 + y^2 \leq R^2$ can be approximated by using the idea shown in

Fig. 2 by introducing m circumscribed squares to generate $4m$ inequality constraints:

$$-R \leq x \leq R, \quad -R \leq y \leq R \quad (28)$$

$$-\frac{R}{\sin \theta} \leq y - \cot \theta \leq \frac{R}{\sin \theta} \quad (29)$$

$$-\frac{R}{\cos \theta} \leq y + \tan \theta \leq \frac{R}{\cos \theta} \quad (30)$$

$$\theta = \frac{k\pi}{2m}, \quad m > 1, \quad k = 1, \dots, m-1 \quad (31)$$

Therefore, each distribution line power flow limit described by (11) can be approximated as a series of linear inequalities:

$$h(P_{ij}, Q_{ij}) \leq 0 \quad (32)$$

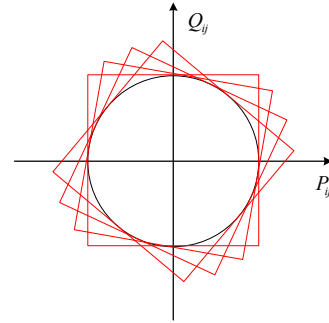


Fig. 2. Polyhedral outer approximation of a power circle

C. Efficient Ad-CG Algorithm for Solving the RTDR

All the polyhedral approximations given above are strictly convex relaxations. The solution space of the RTDR formed by these polyhedrons contains all feasible operating points.

In summary, the RTDR after tight convex relaxation can be expressed as

$$W^{\text{TCR}} = \{\Delta \mathbf{w} \mid \exists \mathbf{y} : \mathbf{B}\mathbf{y} + \mathbf{C}\Delta \mathbf{w} \leq \mathbf{b}\} \quad (33)$$

where \mathbf{y} includes all power flow variables and auxiliary variables except \mathbf{p}^g , \mathbf{q}^g and $\Delta \mathbf{w}$. The linear constraints in (33) include (2)-(4), (6)-(10), (12), (24), (25), and (32). Hereby W^{TCR} is a high-dimensional polyhedron. Solving W^{TCR} involves projecting the high-dimensional polyhedron on the hyperplane of $\Delta \mathbf{w}$. By taking the dual form of the linear constraints related to \mathbf{y} , (33) is equivalent to the following polyhedron [4]:

$$W^{\text{TCR}} = \{\Delta \mathbf{w} \mid \mathbf{u}^T \mathbf{C} \Delta \mathbf{w} \geq \mathbf{u}^T \mathbf{b}, \forall \mathbf{u} \in \text{vert}(U)\} \quad (34)$$

where $U = \{\mathbf{u} \mid \mathbf{B}^T \mathbf{u} = 0, -1 \leq u_i \leq 1\}$. The polytope U has a finite number of vertices, and its coefficient matrix \mathbf{B} is only related to the structure of the power system. U is independent of the current operating condition and is fixed for every given system. Therefore, the specific expression of (34) can be obtained by enumerating the vertices of U .

In small-scale power systems, the vertices of U can be calculated offline in advance. However, vertex enumeration produces a large number of redundant constraints and is

computationally intensive. Enumerating all the vertices of U is not practically possible for a practical-scale system.

The Ad-CG algorithm developed in [4] is employed to identify the binding vertices in U and adaptively generate the boundary of W^{TCR} without seeking any boundary points. In this algorithm, a sufficiently large initial set $W^B \supseteq W^{\text{TCR}}$ is first generated. Then, the algorithm finds all points that satisfy $\Delta w^* \notin W^{\text{TCR}}$ and creates corresponding cut plane constraints to iteratively join W^B until $W^B \subseteq W^{\text{TCR}}$, which means $W^B = W^{\text{TCR}}$. The details of the Ad-CG algorithm are summarized as follows:

Algorithm 1 Ad-CG algorithm to calculate the RTDR

1: Choose a tolerance $\delta > 0$ and a sufficiently large set $W^B = \{\Delta w \mid H\Delta w \geq h\}$. Set $R = +\infty$.

2: While $R > \delta$, solve the following MILP problem:

$$\begin{aligned} R &= \max \mathbf{u}^T \mathbf{b} + \boldsymbol{\zeta}^T \mathbf{h} \\ \text{s.t. } & \mathbf{C}^T \mathbf{u} + \mathbf{H}^T \boldsymbol{\zeta} = 0 \\ & -M\boldsymbol{\theta} \leq \mathbf{h} - \mathbf{H}\Delta w \leq 0 \\ & -M(1-\boldsymbol{\theta}) \leq \boldsymbol{\zeta} \leq 0 \\ & \mathbf{u} \in U, \boldsymbol{\theta} \in \{0,1\}^N \end{aligned} \quad (35)$$

The optimal solution is $(\mathbf{u}^*, \Delta w^*)$, and the optimal value is R . The decision variables of the MILP problem in step 2 include REG forecast error Δw and dual variables \mathbf{u} and $\boldsymbol{\zeta}$. The number of inequality constraints in W^B is N . The vector $\boldsymbol{\theta}$ includes N binary variables, and M is a sufficiently large constant.

3: If $R \leq \delta$, terminate, and report $W^{\text{TCR}} = W^B$; else add the following constraint into W^B :

$$(\mathbf{u}^*)^T \mathbf{C}\Delta w \geq (\mathbf{u}^*)^T \mathbf{b} \quad (36)$$

update matrix \mathbf{H} and vector \mathbf{h} in W^B , and return to step 2.

IV. CASE STUDIES

The performance of the proposed model is tested under a modified IEEE 33-bus distribution system, as shown in Fig. 3. To simplify the structure diagram, some buses and connections are represented by dashed lines. Two distributed energy sources W12 and W26 are added at buses #12 and #26, respectively. The up/down ramping limit of each traditional generator is set to 25% of its capacity. All numeric experiments are conducted on a desktop computer with an Intel i5-8500 CPU and 8 GB memory. All MILP problems are solved by Gurobi 9.10.

To verify the effectiveness of the proposed method in approximating and calculating the RTDR, we compare the following three methods:

1) Exact RTDR (W) determined by system feasible points. By using the MATPOWER program [24] to sample and

calculate in the parameter space Δw , these optimal power flow (OPF) feasible points based on AC power flow can be obtained.

- 2) Linearized approximation RTDR (W^{LA}) proposed in [14].
- 3) Tight convex relaxation RTDR (W^{TCR}) given by (33).

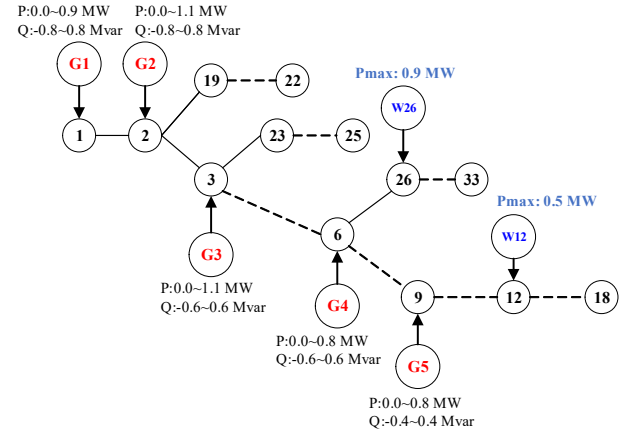


Fig. 3. Modified IEEE 33-bus distribution system structure and generator parameters

A. Performance of the Proposed RTDR

Given the current system state ($W12=W26=0$ MW), the RTDRs of the system obtained by the three methods are shown in Fig. 4. After taking the sampling point interval as 0.03, the red lattice representing the exact W in Fig. 4 can be obtained. Compared with the exact W , the proposed W^{TCR} can completely cover W , and it only contains a small number of infeasible points. This validates that the polyhedron W^{TCR} is a tight convex relaxation of the real RTDR. Meanwhile, W^{LA} using linearized power flow can also contain all of W , but it produces a larger region containing more infeasible points.

The convergence performance in constructing W^{LA} and W^{TCR} is shown in Fig. 5. For the 33-bus distribution system, both methods converge to the predefined accuracy. The linearized model proposed in [14] only needs 17 iterations to converge because it has fewer constraints and variables. The CH relaxation model proposed in this paper introduces more auxiliary variables and outer approximation constraints, but it also converges in 28 iterations.

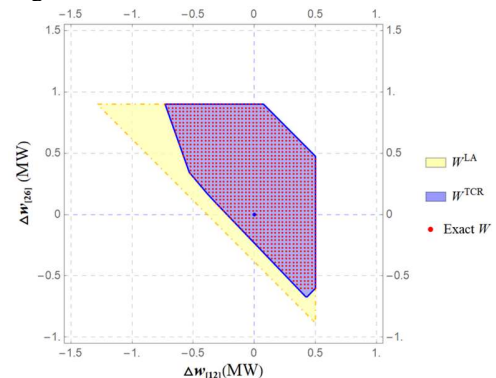


Fig. 4. Comparison of three different RTDRs

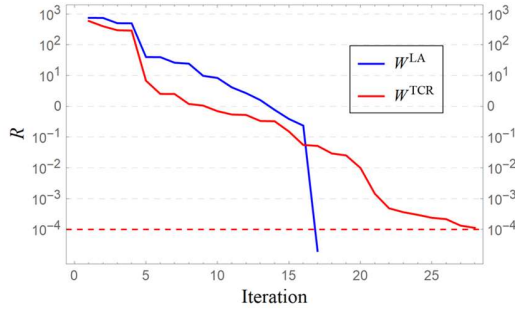


Fig. 5. Performance in calculating W^{LA} and W^{TCR}

B. Impact of the r/x Ratio of Lines

The resistance of each feeder in the distribution system is increased by 50%, and the RTDRs obtained by the three methods are shown in Fig. 6. Increasing the feeder resistance significantly increases the system transmission loss and the voltage drops along the lines. Therefore, the exact RTDR shrinks.

W is a nonconvex region. Comparing W^{TCR} and W , there are some infeasible points near the maximum output of W12. For example, (0.5, 0.68) is an infeasible point in W^{TCR} , which reverses the power flow on the line from bus #8 to #9 and violates the ramping limits of G4 and G5. In this scenario, the active power of G1 and G3 and the reactive power of G2 and G3 reach the upper bound, which violates the first sufficient condition and leads to an infeasible convex relaxation solution.

Meanwhile, W^{LA} cannot contain W after the resistance is increased and includes more infeasible points. W^{LA} cannot adapt to high r/x ratio networks.

The RTDRs with the line resistance increased and decreased by 50% are compared in Fig. 7. An increase (decrease) in the line resistance causes a contraction (expansion) of W^{TCR} .

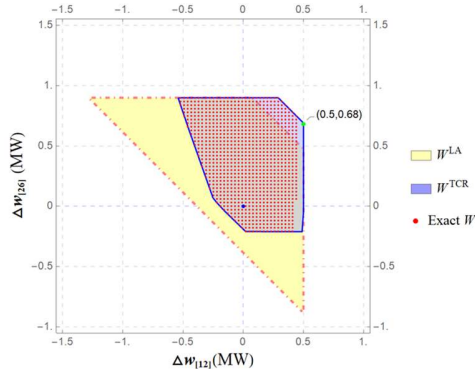


Fig. 6. RTDRs with a 50% increase in the line resistance

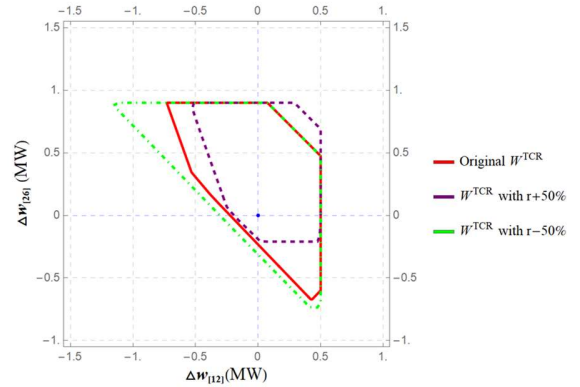


Fig. 7. Influence of different line resistances on the RTDR

In the next case, the RTDR shown in Fig. 8 with a 33% reduction in line reactance has the same r/x ratio as in Fig. 6. Both W^{LA} and W^{TCR} can contain all the exact W . Compared to that in Fig. 6 with a larger resistance, the W^{TCR} in Fig. 8 with a smaller reactance contains fewer infeasible points.

The RTDRs for increased and decreased line reactance by 33% are compared in Fig. 9. As the branch reactance decreases, the active and reactive transmission losses in each feeder decrease, resulting in a larger RTDR.

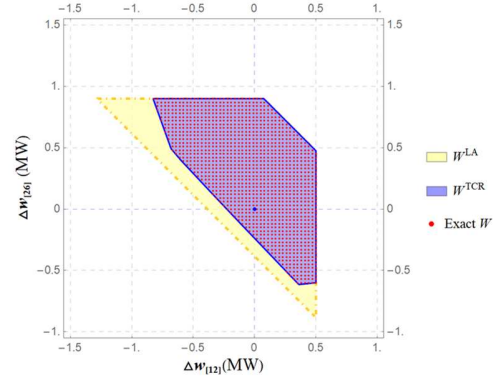


Fig. 8. Results of a 33% reduction in the line reactance

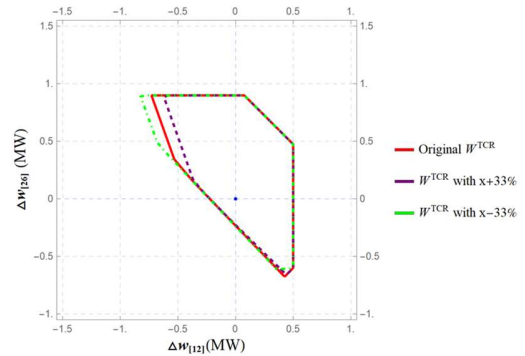


Fig. 9. Influence of different line reactances on the RTDR

C. Impact of the Reactive Load

The RTDRs with a 25% reduction in the reactive load are shown in Fig. 10. The RTDRs for increased and decreased reactive loads are compared in Fig. 11. In this case, W^{TCR} can still cover all the exact W with only a few infeasible points.

The change in system reactive load mainly affects the reduction margin of W1 at bus #12. The reduction in the reactive load can increase the reserve capacity of the reactive power to improve the ability of the system to maintain the voltages at buses #10 to #18.

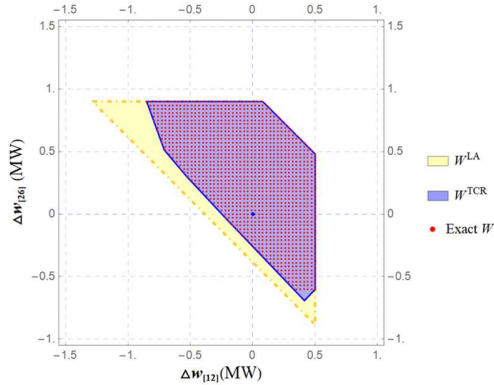


Fig. 10. Results of a 25% reduction in the reactive load

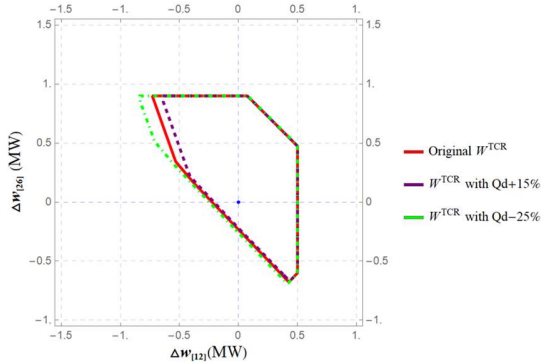


Fig. 11. Influence of different reactive loads on the RTDR

D. Impact of Ramping Limits

In RTD, the system scheduling interval is short, so the ramping constraints of traditional generators cannot be ignored. The W^{TCR} with and without ramping limits are shown in Fig. 12. The comparison of RTDRs reveals that the existence of ramping constraints limits the output of REG to a large increase or decrease at the same time. Moreover, since the line power flow cannot be reversed, increased power generation by W26 cannot support the lines between buses #6 and #18, and the existing ramping capacity of the system cannot withstand a large reduction in W12.

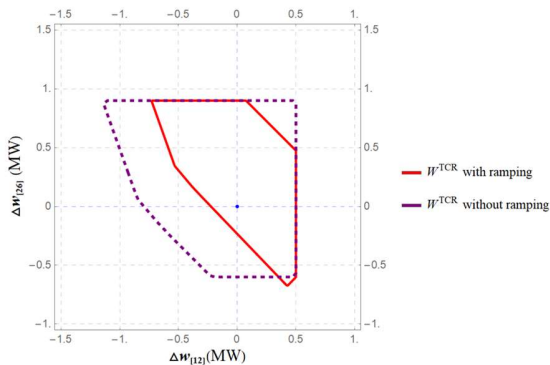


Fig. 12. Comparison of results with and without ramping limits

The Ad-CG algorithm is a polyhedral projection algorithm whose calculation accuracy is related to the value of M , the number of constraints, and the coefficients of constraints. At the vertex in the direction in which the output of W26 decreases, the W^{TCR} with ramping has a smaller protruding region than W^{TCR} without ramping. The protruding region is a set of infeasible points, and the method proposed in this paper cannot provide a definite elimination method at this time. However, the proposed method has sufficient accuracy and computational efficiency to meet the needs of online scheduling and RTD.

E. Larger-scale Case

REG W16 is added at bus #16 with a maximum output of 0.2 MW. The resultant W^{TCR} and the exact W are shown in Fig. 13. The red dots represent the exact RTDR based on the exact AC power flow. The proposed tight convex relaxation RTDR completely contains the exact RTDR. A small number of infeasible points are concentrated on the vertex in the W12 reduction direction. Overall, the proposed W^{TCR} is a good approximation of the exact W .

The performance in calculating the three-dimensional W^{TCR} is shown in Fig. 14. In a 33-bus distribution system, the proposed method converges in 46 iterations, which takes less than 30 seconds, meeting the computational efficiency requirements of RTD.

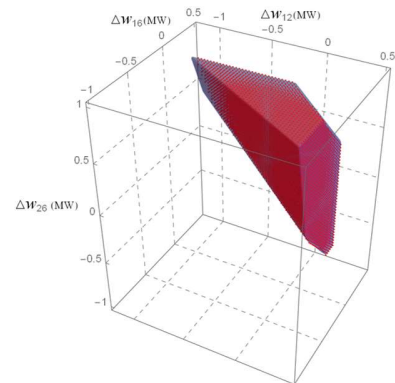


Fig. 13. W^{TCR} (blue) containing the exact W (red dots)

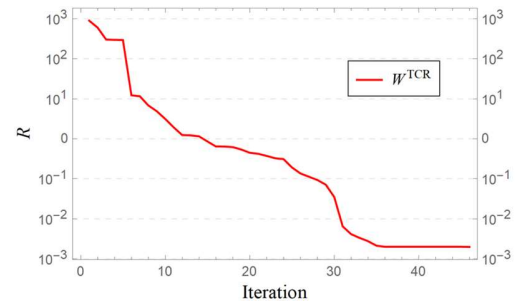


Fig. 14. Performance in calculating three-dimensional W^{TCR}

V. CONCLUSION

This paper proposes an RTDR model in distribution network using the CH of BFM power flow. The proposed model is the tightest convex outer approximation of the actual RTDR, which

is used to accurately describe the ability of the distribution system to hedge the fluctuations of renewable energy. A polyhedral projection method is introduced to obtain a high-precision linear convex outer approximation of the SOC constraint in the CH. The efficient Ad-CG algorithm is used to calculate the boundary of our RTDR.

Numerical experiments are conducted on a modified IEEE 33-bus distribution system. The proposed RTDR is a fairly accurate approximation of the exact RTDR. The calculation and accuracy performance in different cases shows that the proposed method meets the requirements of online applications and RTD. The proposed method provides accurate security boundaries of the distribution system under uncertain injections, and the system operators can use the RTDR to analyze the security margin of the power grid in real time.

REFERENCES

- [1] W. Wei, N. Li, J. Wang and S. Mei, "Estimating the probability of infeasible real-time dispatch without exact distributions of stochastic wind generations," *IEEE Trans. Power Syst.*, vol. 31, no. 6, pp. 5022-5032, Nov. 2016.
- [2] J. Li, F. Liu, Z. Li, C. Shao and X. Liu, "Grid-side flexibility of power systems in integrating large-scale renewable generations: A critical review on concepts, formulations and solution approaches" *Renew. Sustain. Energy Rev.*, vol. 93, pp. 272-284, Oct. 2018.
- [3] W. Wei, F. Liu and S. Mei, "Dispatchable region of the variable wind generation," *IEEE Trans. Power Syst.*, vol. 30, no. 5, pp. 2755-2765, Sept. 2015.
- [4] W. Wei, F. Liu and S. Mei, "Real-time dispatchability of bulk power systems with volatile renewable generations," *IEEE Trans. Sustain. Energy*, vol. 6, no. 3, pp. 738-747, July 2015.
- [5] W. Wei, J. Wang and S. Mei, "Dispatchability maximization for co-optimized energy and reserve dispatch with explicit reliability guarantee," *IEEE Trans. Power Syst.*, vol. 31, no. 4, pp. 3276-3288, July 2016.
- [6] J. Zhao, T. Zheng and E. Litvinov, "Variable resource dispatch through do-not-exceed limit," *IEEE Trans. Power Syst.*, vol. 30, no. 2, pp. 820-828, March 2015.
- [7] Z. Li, F. Qiu and J. Wang, "Data-driven real-time power dispatch for maximizing variable renewable generation," *Applied Energy*, vol. 170, no. 1, pp. 304-313, May 2016.
- [8] D. Bertsimas, E. Litvinov, X. A. Sun, J. Zhao and T. Zheng, "Adaptive robust optimization for the security constrained unit commitment problem," *IEEE Trans. Power Syst.*, vol. 28, no. 1, pp. 52-63, Feb. 2013.
- [9] Y. Guan and J. Wang, "Uncertainty sets for robust unit commitment," *IEEE Trans. Power Syst.*, vol. 29, no. 3, pp. 1439-1440, May 2014.
- [10] J. Qiao, T. Pu and X. Wang, "Renewable scenario generation using controllable generative adversarial networks with transparent latent space," *CSEE J. Power Energy Syst.*, vol. 7, no. 1, pp. 66-77, Aug. 2021.
- [11] X. Zheng, H. Chen, Y. Xu, Z. Li, Z. Lin and Z. Liang, "A mixed-integer SDP solution to distributionally robust unit commitment with second order moment constraints," *CSEE J. Power Energy Syst.*, vol. 6, no. 2, pp. 374-383, June 2020.
- [12] Z. Chen, G. Zhu, Y. Zhang, T. Ji, Z. Liu, X. Lin and Z. Cai, "Stochastic dynamic economic dispatch of wind-integrated electricity and natural gas systems considering security risk constraints," *CSEE J. Power Energy Syst.*, vol. 5, no. 3, pp. 324-334, Sept. 2019.
- [13] X. Qin, X. Shen, Y. Guo, Z. Pan, Q. Guo and H. Sun, "Combined electric and heat system testbeds for power flow analysis and economic dispatch," *CSEE J. Power Energy Syst.*, vol. 7, no. 1, pp. 34-44, Jan. 2021.
- [14] Y. Liu, Z. Li, Q. H. Wu and H. Zhang, "Real-time dispatchable region of renewable generation constrained by reactive power and voltage profiles in AC power networks," *CSEE J. Power Energy Syst.*, vol. 6, no. 3, pp. 528-536, Sept. 2020.
- [15] Q. Li, R. Ayyanar and V. Vittal, "Convex optimization for DES planning and operation in radial distribution systems with high penetration of photovoltaic resources," *IEEE Trans. Sustain. Energy*, vol. 7, no. 3, pp. 985-995, July 2016.
- [16] H. D. Nguyen, K. Dvijotham and K. Turitsyn, "Constructing convex inner approximations of steady-state security regions," *IEEE Trans. Power Syst.*, vol. 34, no. 1, pp. 257-267, Jan. 2019.
- [17] D. Lee, H. D. Nguyen, K. Dvijotham and K. Turitsyn, "Convex restriction of power flow feasibility sets," *IEEE Trans. Control Netw. Syst.*, vol. 6, no. 3, pp. 1235-1245, Sept. 2019.
- [18] M. Farivar and S. H. Low, "Branch flow model: relaxations and convexification—Part I," *IEEE Trans. Power Syst.*, vol. 28, no. 3, pp. 2554-2564, Aug. 2013.
- [19] M. Farivar and S. H. Low, "Branch flow model: relaxations and convexification—Part II," *IEEE Trans. Power Syst.*, vol. 28, no. 3, pp. 2565-2572, Aug. 2013.
- [20] Q. Li and V. Vittal, "Convex hull of the quadratic branch AC power flow equations and its application in radial distribution networks," *IEEE Trans. Power Syst.*, vol. 33, no. 1, pp. 839-850, Jan. 2018.
- [21] S. H. Low, "Convex relaxation of optimal power flow—Part II: Exactness," *IEEE Trans. Control Netw. Syst.*, vol. 1, no. 2, pp. 177-189, June 2014.
- [22] A. Ben-Tal and A. Nemirovski, "On polyhedral approximations of the second-order cone," *Math. Oper. Res.*, vol. 26, no. 2, pp. 193-205, May 2001.
- [23] F. Glineur, "Computational experiments with a linear approximation of second-order cone optimization," 2000.
- [24] R. D. Zimmerman, C. E. Murillo-Sánchez and R. J. Thomas, "MATPOWER: Steady-state operations, planning, and analysis tools for power systems research and education," *IEEE Trans. Power Syst.*, vol. 26, no. 1, pp. 12-19, Feb. 2011.